Available online at www.sciencedirect.com

ScienceDirect

Physics Procedia 90 (2017) 242 – 255

Physics Procedia

Conference on the Application of Accelerators in Research and Industry, CAARI 2016, 30 October – 4 November 2016, Ft. Worth, TX, USA

Vehicle and Cargo Scanning for Contraband

Joseph Bendahan[a]*

[a]*Rapiscan Laboratories, Inc., 520 Almanor Ave., Sunnyvale, CA 94085, USA*

Abstract

There is a need to inspect vehicles and their contents for Special Nuclear Material (SNM) and general contraband. The most widely used technology for scanning vehicles, ranging from vans and trucks to railcars, is gamma-ray and X-ray radiography. New technologies are required for higher penetration to reduce insufficient penetration alarms, for improved image quality and material discrimination to increase detection at high throughput and to enable scanning fast-moving trains. In most cases, the scanning footprint, which includes the radiation exclusion zone, must be small due to the limited space available at the inspection sites. Some of these conflicting requirements have been addressed by employing adaptive intensity and/or energy modulation of the X-ray source. Any alarms produced by these primary systems need to be cleared or confirmed to eliminate labor-intensive manual inspection. Various technologies have been proposed and used for secondary inspection, mainly based on the detection of fission signatures. Such systems would preferentially require minimal infrastructure and cost would be kept reasonably commensurate with the performance improvements to allow for wide deployment. The Domestic Nuclear Detection Office (DNDO) has performed tests of some of these systems to determine the envelope of the various technologies. Selected results with primary systems, and examples of potential system improvements are presented.

Peer-review under responsibility of the Scientific Committee of the Conference on the Application of Accelerators in Research and Industry

Keywords: Radiography; Special nuclear material (SNM); Contraband detection; Active interrogation; Intensity modulation; Muon detection system.

* Corresponding author. Tel.: +1-408-961-9706; fax: +1-408-727-8748.
E-mail address: jbendahan@rapiscansystems.com

Peer-review under responsibility of the Scientific Committee of the Conference on the Application of Accelerators in Research and Industry
doi:10.1016/j.phpro.2017.09.003

1. Introduction

Cargo containers and rail cargo have been identified as a probable mechanism to smuggle nuclear material into the United States (U.S.). Approximately 32,000 cargo containers arrive in the U.S. ports and 5,400 railcars cross the U.S. borders daily. These numbers are expected to rise with the increase in commerce.

In 2007, Congress passed a mandate requiring that cargo must be scanned using imaging scanners before arriving to the U.S. by 2012. Due to the complexity of the procurement and operational logistics and, to some extent, due to the lack of viable technologies, an extension through 2018 was approved. It has been estimated that it would cost approximately $20 billion to meet the mandate for the 700 foreign ports that ship cargo to the U.S. (Espie, 2016). Therefore, innovative and cost effective approaches are required to ensure container and rail-cargo security.

The U.S. Department of Homeland Security (DHS) Domestic Nuclear Detection Office (DNDO) was tasked by the National and Homeland Security Directives to protect against radiological and nuclear ("RadNuc") threats directed against the U.S. DNDO has been seeking to identify commercially available equipment to meet the requirements to detect threats, regardless of the amount of shielding or the complexity of cargo with minimal impact to the flow of commerce before eventual deployment. As part of the nuclear detection effort, DNDO has funded a number of Advanced Technology Demonstration (ATD) campaigns, including Cargo Advanced Automated Radiographic System (CAARS), Shielded Nuclear Alarm Resolution (SNAR) and Nuclear and Radiological Imaging Platform (NRIP). DNDO has also funded other Exploratory Research Programs (ERPs) for development general aviation and advanced rail- cargo scanners, portable systems, system components and other areas.

Customs and Border Protection (CBP) currently performs inspections for general contraband and radiological materials. CBP employs a protocol called Automated Targeting System (ATS) to identify a percentage of cargo for inspection with imaging scanners (CBP, 2017). Currently, all containers arriving in U.S. ports and border crossings are screened by Radiation Portal Monitors (RPMs), and when an alert surfaces the container is also subject to secondary screening. In light of this, improvements in general contraband and radiological detection are sought for imaging cargo scanners.

2. DNDO Advanced Technology Demonstrations

2.1. Basic Concept of Operations

The basic approach is to use a primary system to inspect cargo at high throughput to identify suspect objects and employ a secondary system to clear or confirm the alarms. It is preferred to employ a single system to detect also nuclear materials. However, material-specific technologies would be required to result in very low alarm rates (<<1%). These techniques are inherently slow or require very high-power sources that would increase exclusion zone, or most probably would require a shielded facility.

A secondary system could be collocated, placed at a distance, or it could be integrated into the primary system, operated in a different mode for the second scan. For low-throughput operations, collocation and using the same system would probably work. However, for high throughput, the secondary system would be placed elsewhere to prevent reducing the throughput of the primary system during the longer scanning time of the secondary inspection.

RPMs are required for the detection of radiological sources, and complement X-ray scanners which cannot directly detect these sources. RPMs are very sensitive and can also be triggered by nearby X-ray scanners. Typically, the RPMs are therefore inhibited during the intense radiation pulse of the linac source used by most cargo scanners. Depending on the system configuration, energy and power, RPMs need to be placed at a safe distance. In any case, the data from the RPM and primary system should be fused to improve detection.

2.2. DNDO-Funded Programs

As mentioned, as part of the nuclear detection effort to develop technologies to protect the U.S. against RadNuc threats, DNDO has funded a number of ATD projects including CAARS, SNAR, and NRIP.

The CAARS program dealt with only radiographic (primary) systems. The SNAR program supported two approaches: Integrated (I-) SNAR and Relocatable (R-) SNAR. The I-SNAR concept consisted of a single integrated primary and secondary system where the cargo was brought back for secondary inspection when the primary system alarmed. The R-SNAR concept consisted of a secondary inspection system that could be easily relocated.

Under the CAARS program, two dual-energy ("DE") systems operating at 6/9 MV interlaced energies were tested (denoted as DE-1 and DE-2 in the next section). A single-energy (6-MV) system was also tested using an automated algorithm (denoted as ASE).

Under the SNAR program, three systems were tested:

1. I-SNAR type system, based on three technologies High-Energy Backscatter (HEB, see Bertozzi et al., 2007, Medalia-1, 2010), Prompt Neutron from Photo Fission (PNPF, see Danagoulian et al., 2010) and Nuclear Resonance Fluorescence (NRF, see Bertozzi et al., 2005);
2. Photofission-Based Alarm Resolution or PBAR system (Stevenson, 2010); and
3. Differential dieAway and PHotofissioN Experiment (DAPHNE).

Under the NRIP program a Muon Tomography (MT-1) system was tested (Medalia-2, 2010, Blanpied et al., 2015). Baseline characterization of commercial systems which integrate passive detection with radiography and/or Automated Threat Recognition (ATR) have also been tested and data are being analyzed (Rynes, 2015).

2.3. Results (Bentley, 2016)

The various systems were tested placing a number of targets and potentially alarming objects, with different shielding configurations, in many positions within a set of varying cargos. Data were collected several times for each configuration to test for reproducibility. The number of cargo inspection test runs for each system ranged from 500 to 5000, with 1,000-12,000 embedded threats. The cargo was divided in four categories with combinations of low ("L") and high ("H") density and clutter. An example of an image from a cargo container is shown in Fig. 1.

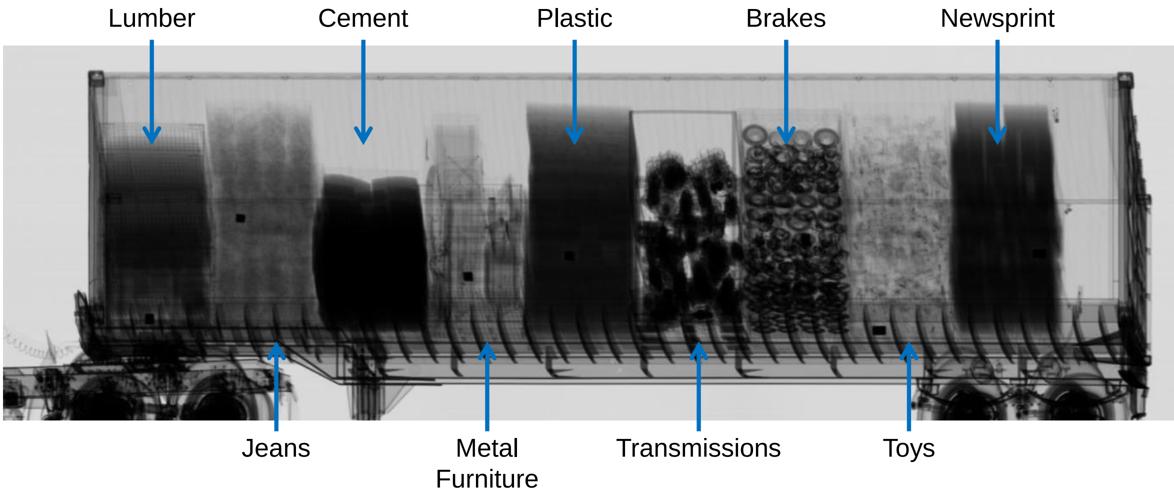

Fig. 1. Examples of cargos employed by DNDO for Advanced Technology Demonstration tests.

After conclusion of the field tests, DNDO provided 50-60% of the data to the vendors for tuning ("Released Data Set") and kept the rest for testing ("Sequestered Data Set"). The images from typical single-energy radiographic systems (MSE) were analyzed manually by operators. The vendors of the dual-energy systems (DE-1 and DE-2) developed proprietary automated algorithms that used dual-energy and other features. The single-energy system (ASE) also employed the automated algorithm. Third party vendors were also given the images collected for some of these systems and developed their own algorithms.

The results for the single-energy systems are shown in Fig. 2, where the x-axis shows the cargo alarm rate with no threats and the y-axis shows the probability of detecting threat objects. Some early results of the tests and spiral development indicate the significant progress in increased detection and lower false alarm rate (moving left and up). The result of third-party developer for automated single energy is also shown for comparison. The third-party performance is significantly lower compared to the ASE algorithm.

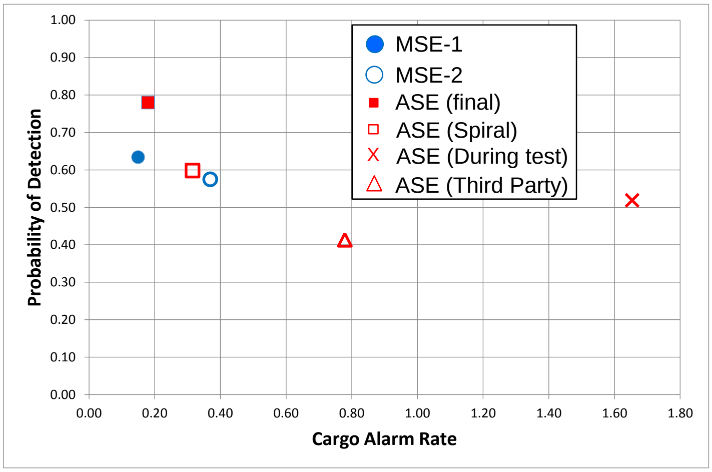

Fig. 2. Comparison of single-energy system performance of DNDO tests.

The results for the dual-energy systems (DE-1 and DE-2) and third-party developers are shown in Fig. 3. The DE-1 vendor developed two algorithms: physics based and machine learning, with the latter algorithm performing better. The DE-2 vendor tuned the algorithm for two points on the Receiver Operating Characteristic (ROC) curve. As expected, the false alarm rate went down, so did the detection rate. The third-party algorithm developer performed better for both vendors than the vendors' algorithms (indicated with * in Fig. 3).

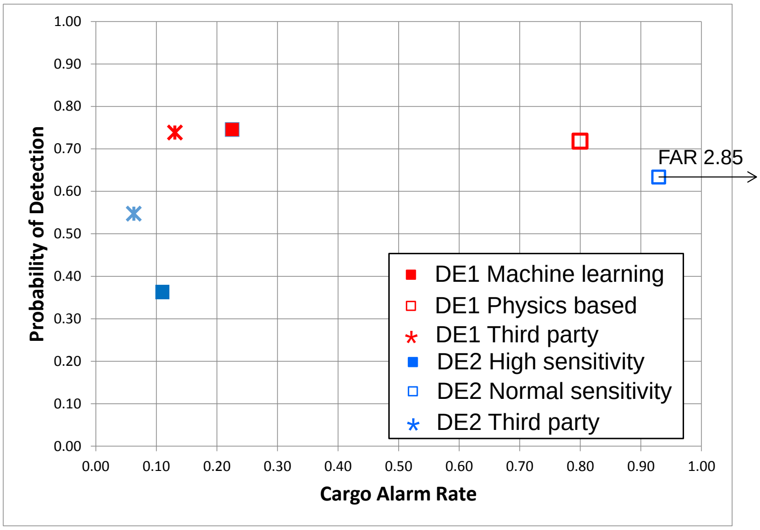

Fig. 3. Comparison of DE-1 and DE-2 system performance of CAARS tests.

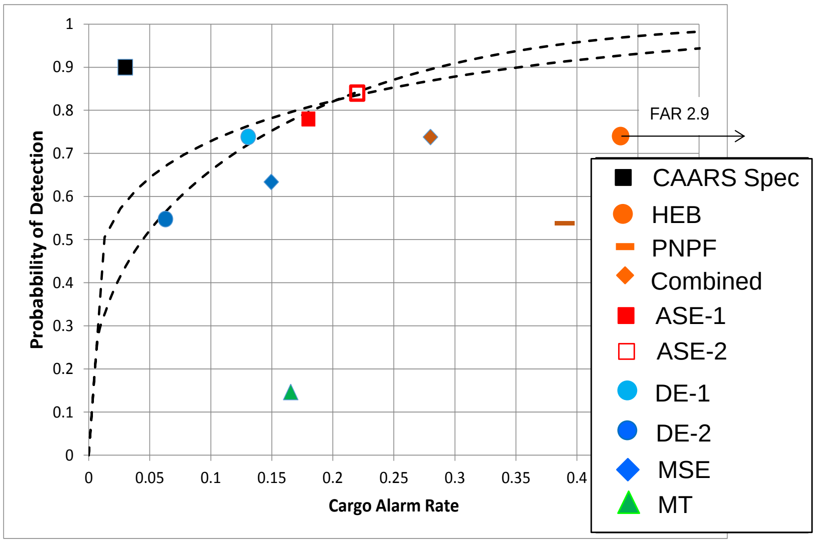

Fig. 4. Performance comparison of the various DNDO tests from primary systems. The dotted lines show a guideline to gauge the approximate trend of the performance for different detection and cargo alarm values.

In Fig. 4, the best results of the previous single and dual-energy tests are shown with the results of the Muon Tomography (MT) system, HEB, PNPF and the HEB-PNPF data fused. Two different results of the ASE algorithm are presented to show the performance trend. The dotted curves are included to indicate approximate ROC curves where the systems performance is equivalent if they were tuned to different detection and cargo alarm set points.

The ASE and DE-1 third-party algorithms seem to have the highest performance. Depending on the actual ROC curve, the DE-2 third-party algorithm may have similar or lower performance. Note that the system, to which the ASE algorithm was applied uses single-energy (6 MV) images, has a small exclusion zone with no building and has a high throughput of 180 trucks/hour. Although the ASE algorithm has been applied only to single-energy images during the DNDO tests, preliminary analysis of dual-energy images show indications that a dual-energy algorithm extension could further increase performance.

HEB-PNPF data-fused and the Manual Single Energy followed in performance. Although the performance of the Manual Single Energy was low, it indicates that operator analysis might be useful, for example, as second-level inspection. The muon-tomography (MT) system performed quite poorly in primary (2-min scanning time), as the number of available muons is low. Higher performance was obtained for longer times, but the throughput is too low for primary inspection.

Analysis of the data from the SNAR tests has not been completed and will be reported once available.

3. Advanced Designs

The DNDO tests have been targeted to trucks and sea cargo containers. However, there is also a need to inspect railcars that can hold denser and wider cargo. Also, there is a need to improve the primary detection performance at higher throughput to reduce the impact to the flow of commerce and allow for 100% cargo scanning. A small exclusion zone must be maintained to make systems suitable for operation at the sites where they are deployed.

These improvements require optimizations in various areas including:

- Beam energy, single/dual or multiple energies;
- Advanced detectors;
- Improved configurations;
- Advanced scanning approaches.

Examples of improvements in these areas are described below.

3.1. Beam Energy and Power

The selection of the beam energy and power significantly affects the characteristics of radiographic inspection systems. The imaging penetration increases with energy, but so do the system cost and radiation footprint. A tradeoff between these factors is performed based on specific customer requirements. For example, for mobile applications, a small radiation footprint (typically 120ft x 140ft) and a low-weight vehicle is very important. Since higher-energy and higher-power X-ray sources would increase the vehicle weight and the exclusion zone, low energy (< 6 MV) and low beam power (~ 10W) are used, resulting in a relatively low penetration.

Most commercial scanners employ pulsed linacs with interlaced dual-energy (4/6 MV) beams to allow for some material discrimination. These can have a beam power up to about 0.6kW when running at 100μA. There are some deployed scanners that employ 9 MV linacs with beam power up to almost 1kW. The beam energy for radiography to detect SNM and general contraband with high detection performance should be at least 6 MV to allow for penetration of most cargos. A higher energy of 9-10 MV and higher power (> 1kW) is preferred, especially for rail cargo scanning.

Sources with power above 1kW have been used mainly for industrial applications, such a sterilization, food irradiation, etc. These sources are more expensive than the commercially available linacs used for security inspection applications. Recently, DNDO has issued BAA HSHQDN-16-R-0002 to develop high-power sources at an affordable price in anticipation of the next-generation of scanners. However, some end users have started using lighter mobile scanners with reduced exclusion zone required at some sites. These requirements result in lower penetration with the consequence of increased dark alarms (insufficient penetration) and make SNM detection more difficult.

3.2. Beam Pulsing

Pulsed X-ray linacs are the most widely deployed sources for security inspection due to their relative compactness, the range of available energies and power, and their relatively lower cost. Most linacs deployed for security inspection applications employ magnetrons due to their lower cost and because unlike medical equipment, security inspection systems are more price-sensitive. Magnetrons limit the beam duty cycle to < 0.1%, with pulse widths < 5μs at a pulse rates < 400 pulses per second (pps).

Higher pulse rates would benefit high-speed railcar inspection, in particular, if they support dual-energy scanning and certain other scanning modes. e2V produces a solid-state magnetron modulator ("model AMM2") that can reach 1kHz pulse rate. Higher rates are possible by using klystrons (Condron, 2013), but their higher cost has hindered deployment in security applications. SLAC has designed highly efficient, low-cost, compact, low-voltage (~60kV) and high-duty-factor devices that hold promise to scale up to a higher power at a reasonable cost (Tantawi, 2015).

Continuous Wave (CW) sources enable certain types of applications that require single-photon counting techniques. For example, Passport Systems' EZ3D and PNPF techniques measure the spectra of gamma rays and neutrons. Rapiscan's Transmission Spectroscopy (Z-SPEC) would benefit greatly from using CW (or high-duty) sources to allow measuring the transmitted X-ray spectrum with sufficiently low pileup to determine the Z of cargo. CW sources are typically more complex, larger and more expensive than pulsed linacs, which have limited CW sources deployment. Under the Exploratory Research (ER) Broad Agency Announcement (BAA) solicitation No. HSHQDN-16-R-0002, DNDO is also requesting development of low-cost CW sources to enable some technologies.

3.3. Material Discrimination

Material discrimination for general contraband and SNM detection is required. The most widely used method for material discrimination is dual-energy scanning (Ogorodnikov et al., 2002). However, SNM can be detected with single-energy radiography using algorithms such as ASE algorithm, as shown in the DNDO tests described above. More recent methods include multi-energy scanning (Arodzero, 2015), EZ3D, Transmission Spectroscopy (Z-SPEC, Gozani et al., 2014, Langeveld et al., 2012), and Noise Spectroscopy (Z-SCAN, Langeveld et al., 2011, 2013). Multi-energy scanning requires new sources capable of switching energy quickly and associated fast detectors and electronics. EZ3D employs high-power CW sources with an electron-beam steering system and an array of collimated spectroscopic detectors. Z-SPEC requires either CW or high-duty sources (ideally $\geq 5\%$) with fast spectroscopic transmission detectors. Noise Spectroscopy can be used with commercially available linacs, but also requires moderately fast detectors with digitizers. Also, most of these technologies work significantly better at higher energies.

Although dual-energy scanning does not have some of the advantages of the above other techniques, it is the simplest and lowest cost material-discrimination method available and may stay as the preferred method for years to come.

3.4. System Penetration

When part of the image is dark ("insufficient penetration"), the system produces an alarm, which in an automated (or "operator-assist") threat recognition system is added to the list of alarms that require a secondary scan or manual labor. Higher alarm rates require a large infrastructure, disrupt the flow of commerce and are expensive to handle. The lack of penetration is a greater issue for rail cargo primarily systems due to the higher cargo density.

To determine the penetration requirements, Rapiscan analyzed a database for rail cargo entering the U.S.. The results show that the majority of thr cargos could be inspected with existing high-end X-ray rdiographic systems. However, the rest requires significantly higher penetration capability. This high-penetration requirement could be addressed using other approaches, such as a "known shipper program" where certain cargos are not as carefully inspected because the shipper has been previously thoroughly vetted.

High-performance 6 / 9 MV radiographic portal systems can achieve a penetration of approximately 43cm of steel. However, penetration drops for rail scanners as the scanning speed increases and because usually, the source-to-detector distance is larger therefore, there is a need to increase penetration further.

Traditional methods to increase penetration include collimation (to reduce scatter) and higher energy and/or higher power. However, the energy cannot be increased above 10MV due to World Health Organization limitations (WHO, 1990), and the issue of associated large exclusion zones or otherwise the need for radiation protection infrastructure. Higher power requires higher-cost sources and penetration improvement reaches a plateau at some point due to scatter.

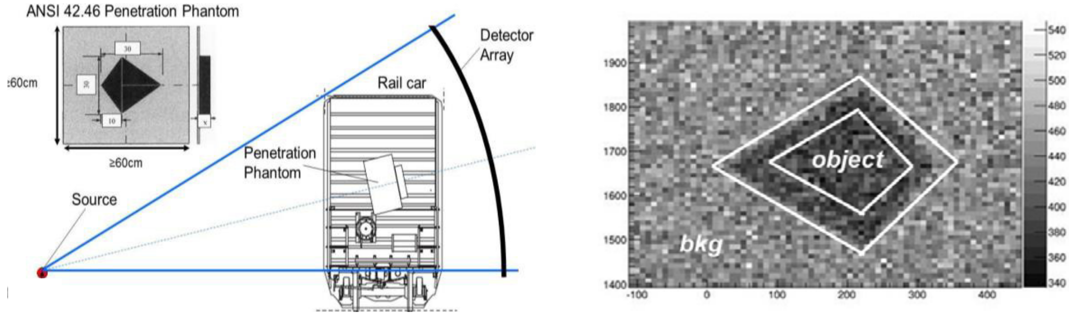

Fig. 5. ANSI penetration phantom and placement within the object (railcar in this case) – left; radiograph of the phantom showing the areas where the object and background mean counts are computed.

3.5. System Optimization

Simulation is one of the existing methods that can be used to optimize system parameters to improve penetration. In particular, Figure 5-left shows the simulated system performance of the ANSI 42.46 penetration phantom. The approach consists of determining the penetration in a quantitative way by computing the Contrast-to-Noise (CNR) ratio for the penetration phantom with the goal of maximizing the CNR. The CNR is an indicator of the visibility of an object in an image, and a higher CNR indicates a higher likelihood of passing the ANSI penetration test.

The CNR of an object in the image depends on the mean value of the object image and background (see Figure 5-right). The edge region of the arrow object is neglected in the calculation. The calculation method for CNR is given below:

$$CNR = \frac{< bkg > - < object >}{\sqrt{\sigma_{bkg}^2 + \sigma_{object}^2}} \quad [1]$$

Below we will discuss three applications to demonstrate the optimization approaches for collimator design, air-gap optimization, and energy thresholding.

3.5.1. Detector Collimator Optimization

Detector collimators are characterized by two main parameters: depth and septum wall thickness. Deeper collimators are expected to reject more scatter as the scattered X-rays traverse more material, however, the collimator cost increases. The situation is similar with using thicker walls; however, the transmitted signal is also reduced. To determine the tradeoffs in these parameters, simulations were performed with different depths and wall thickness.

The simulation results are shown in Fig. 6. The columns show simulated radiographs for several (relative) linac powers and the rows show images for collimator depths from 0mm (i.e., no collimators) to 300mm. The CNR values are shown on the left of each radiograph; an error of ±10-20% is estimated. As expected, the CNR increases with linac power as the statistical noise goes down. For a fixed power, the CNR increases as the collimator depth is increased with small improvements from 200mm to 300mm, which shows that an optimum depth is close to 200mm. A similar analysis was performed for the wall thickness optimization (not shown).

3.5.2. Air-gap optimization

We also evaluated another option to reduce sensitivity to container scatter, known as the “air-gap” method. This method simply consists of moving the detector array further back from the object under inspection. By increasing this gap, the detector-observed scatter is reduced because the scatter contribution falls faster than the signal loss due to increased source-to-detector distance.

Simulations were performed with the configuration shown in Fig. 5 using a 9-MV X-ray beam. The energy spectra of the X-rays at the detector face are shown in Fig. 7-left for several air-gap distances beyond the nominal distance. The spectra are limited to the geometric extent of the detectors shadowed by the penetration object, and so these detectors are occluded from the direct beam. The spectra for each air gap are given separately for the contribution from direct un-scattered transmission through the penetration object and for the contribution from scatter. The transmission spectra are scaled by 10x to be visible on the same scale as the scatter. The discrimination between scatter and transmission was made by cutting on the incident angle of the X-rays at the detector face relative to the detector face normal.

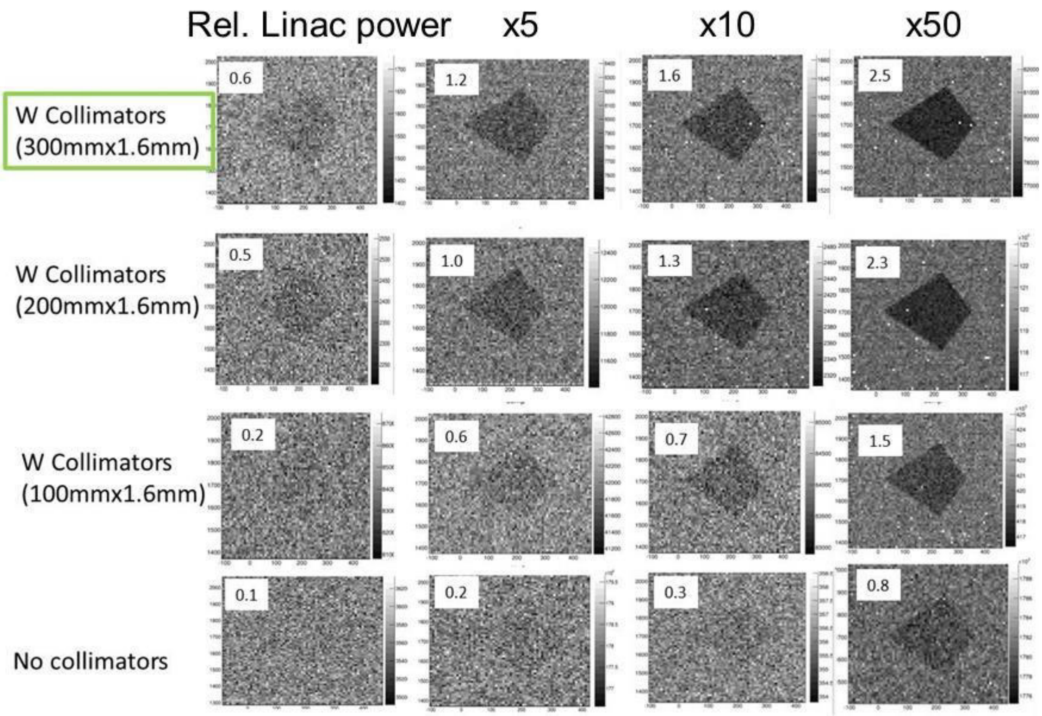

Fig. 6. 600mm penetration of steel using a flux of 9MeV Bremsstrahlung X-rays for different detector collimator lengths. CNR score is shown in the top left of each image.

The simulations were extended to transport the X-rays in 30mm-deep $CdWO_4$ crystals. The X-rays deposit part of the energy in the crystal, while the other part is carried away by Compton scattering. Although the distribution shown in Fig.7-right has a larger overlap, there is still a significant separation.

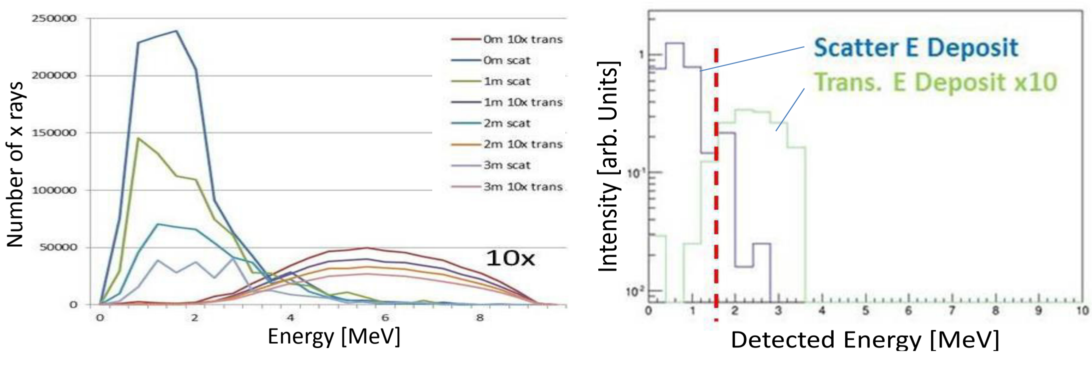

Fig. 7. X-ray spectra behind the penetration object, separated into scatter and transmission components incident on the face of the detector for several air-gap distances (left) and detected by the 30mm-deep $CdWO_4$ crystal.

The resulting radiographs in Fig. 8 show that there is a steady increase in CNR up to a source-to-detector distance of 3m of additional air gap, beyond which the CNR falls. This result suggests that such an air gap will give the highest penetration, roughly a 30% improvement over the baseline configuration. The results for other configurations with different source-to-cargo and cargo-to-detector distances would vary.

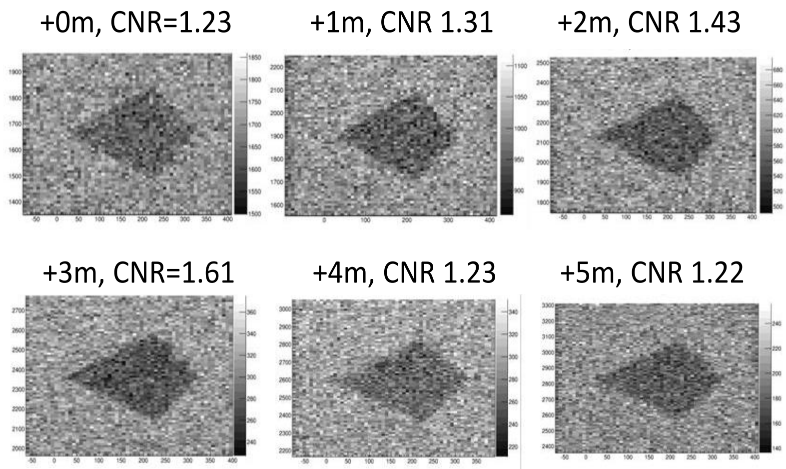

Fig. 8. Contrast-to-noise ratio of the 500mm penetration object for a series of increasing air gap distances at 50kW. The highest CNR is observed at +3m from the base distance.

3.5.3. Advanced Detectors

Simulations were also performed with energy-sensitive detectors to determine the scatter rejection that could be achieved by employing energy thresholding. As shown in Fig. 7, the spectrum of the scattered X-rays is dominated by low energies, while the low-energy transmitted X-rays have been severely attenuated. Fig. 9 shows images of the ANSI penetration phantom for 0, 1 and 2 MeV energy thresholds. The results show the increased CNR as the threshold is increased.

It is important to note that this type of analysis requires single-photon counting, which is possible with CW or high-duty (> 5%) pulsed linacs. Despite having the same power, these sources would provide imaging systems with greater steel penetration ability. However, they would be more costly and may hinder wide deployment.

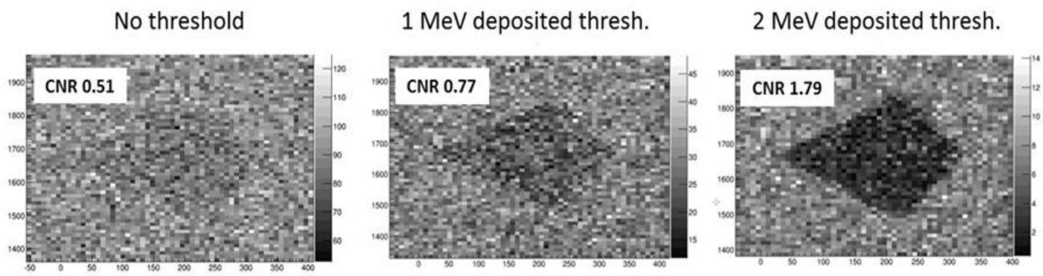

Fig. 9. 500mm radiographs at 10kW at three thresholds on deposited energy in the scintillator.

3.5.4. Intensity Modulation

Use of high-energy X-rays for cargo inspection requires tradeoffs. On one hand, the source needs to produce high-intensity, high-energy X-ray beams to provide high penetration of the cargo. On the other hand, higher X-ray intensities and energies lead to a higher radiation dose and a larger footprint to the cargo inspection systems. A larger controlled area (exclusion zone) around the system or more shielding is required. In the case of portal applications, the driver could potentially be exposed to higher radiation doses.

Until recently, available X-ray sources had one fixed intensity setting set to the output level requested by the customer, typically, the highest setting that still complies with required radiation footprint. This setting is often not the rated maximum intensity of the source.

One solution is to adjust the source intensity based on the observed cargo attenuation (Langeveld, 2009). This approach consists of monitoring the transmitted signals for each pulse in real-time and setting the intensity of the next pulse before it is fired. This approach requires that image data are acquired promptly after the pulse and evaluated, as well as a source capable of changing intensity between one pulse and the next by electronic signal.

Preliminary results have shown up to two inches greater penetration capability while retaining the same radiation footprint as present fixed-intensity sources. Conversely, the penetration could be maintained while reducing the footprint.

Another application of intensity modulation is the capability of scanning the cab of trucks without exceeding the radiation limits to the driver (e.g. Rapiscan CabScan^{TM}). In this approach, the driver cab is scanned with a low-energy, low-intensity X-ray beam and the cargo is scanned using the standard mode. An example of an image of a complete truck scanned in this way is shown in Fig. 10.

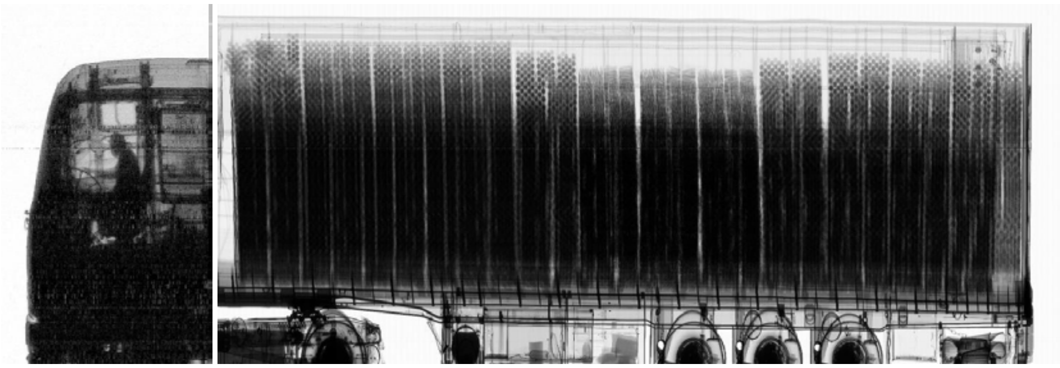

Fig. 10. Image of the complete truck using CabScan where the cab of the truck is scanned at low energy and low intensity without exceeding the radiation dose to the driver, while the rest of the truck is scanned in the standard mode.

3.6. Muon Detection as a Secondary Inspection System

Secondary inspection systems are usually based on active interrogation, where high-energy X-rays and/or neutrons are used to induce fission in SNM with subsequent measurement of the prompt and delayed neutrons and gamma rays. However, some of these systems are costly and complex and require a large footprint. Muon detection is a passive technique that has been demonstrated in a primary system, but with low detection performance due to the poor muon statistics in the allotted time and the existence of cargo-SNM ambiguities.

Muon detection for a secondary inspection has been proposed by Lingacom and Rapiscan (Bendahan, 2014). The approach combines two technologies, an X-ray system that performs high-throughput cargo scanning for general contraband and SNM, and the more-specific muon detection system that serves as a secondary system to resolve alarms.

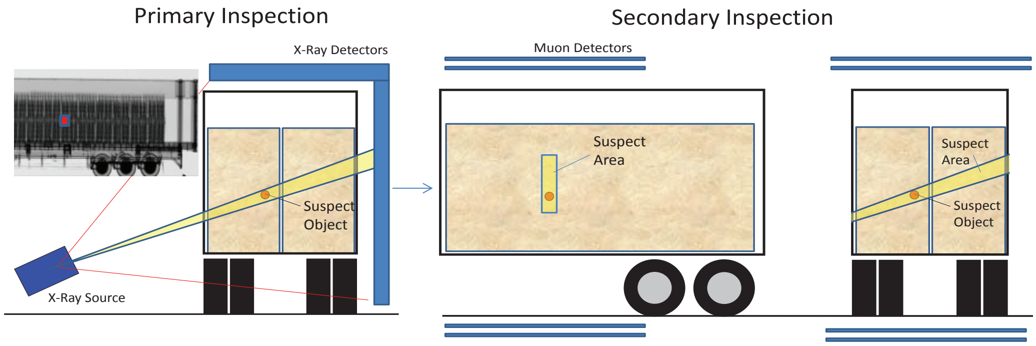

Fig. 11. Primary high-energy inspection system (left) and Secondary Muon Detection System, end view (center) and side view (right).

In the muon detection approach, X-ray images (yielding attenuation and Z information), and the high-Z alarms generated by the X-ray inspection are passed on to the secondary muon inspection system. The cargo is moved so the suspect object is centered at the relatively small (compared to a full system) muon detectors placed above and below the cargo. The results of the passive measurements, the position of the suspect SNM along the X-ray path (yellow area in Figure 11) and the X-ray image data are fused to confirm or clear the presence of high-Z materials.

Muon scatter depends on the cargo materials traversed by the muons between the detectors, resulting in ambiguities for scatter by a large mass of low-medium Z cargo and scatter by high-Z materials. The X-ray system provides valuable information, such as the approximate location of the suspect object, cargo extent, density, and Z, which serve as important constraints to produce accurate muon-scattering images, resulting in higher detection performance according to Geant4 simulations. Another advantage of the combined X-ray and muon detection systems is that specific shapes and configurations could likely be detected by automated and/or operator analysis of the X-ray images. Experimental measurements are planned for summer of 2017 to demonstrate the extent of the improvements.

Such a muon detection system may have other disadvantages. However, the relatively low cost and passive nature of the inspection (no radiation to cargo and no exclusion zone) would enable wide deployment, in particular at sites with limited space. This could be compared to the worldwide deployment of RPMs, despite their known weaknesses.

4. Discussion

DNDO has developed stringent requirements for the detection of nuclear materials due to the catastrophic consequences of not detecting such materials. To this effect, DNDO has supported a number of efforts to develop and test cargo scanning systems with the specific purpose of detecting nuclear materials. There are also other primary missions of enforcement of trade and immigration, which includes protecting the U.S. from all threats. Therefore, there is a need to inspect cargo as part of a customs function, for both manifest verification and the identification of contraband such as narcotics, explosives, weapons and other prohibited items within the limited allocation of scanning infrastructure, constrained resources and funding restrictions; while maintaining the flow of commerce.

Therefore, the selection of imaging scanning systems that would allow for effective 100% inspection of all potential threat items before cargo reaches the U.S., would require a judicious tradeoff between high performance (to meet requirements for contraband detection such as high spatial resolution and low/medium-Z material separation), high throughput, small exclusion zone, simple logistics with low acquisition and operational costs. In order to simultaneously satisfy both missions, equipment must meet the detection capability of both general contraband and nuclear material inspection within the above constraints.

It is very likely that the advanced systems required to detect SNM would be more expensive and would have some impact to the existing logistics. DNDO would like the capability to detect small quantities and various forms of nuclear material that can be used for making a nuclear or radiological device. However, the illicit import of small quantities of SNM would require fabricating a weapon with a usable shape within the U.S. introducing considerable difficulty and the likelihood of exposing additional clues to such plot (Medalia-3, 2010). Thus, exceedingly stringent detection requirements while achieving high detection and very low false alarm rates would result in complex and costly inspection systems that would, therefore, be less likely to be deployed.

A multi-tier approach similar to the one taken by the Transportation Security Administration (TSA) for the detection of explosives is suggested. TSA would also like the capability to detect extremely small and thin explosives, including the home-made explosives or HME (S&T, 2016). However, TSA understands that requiring this level of detection would result in unacceptably high false-alarm rates. Instead, TSA has used a tiered approach over time, requiring a well-defined increasing performance of detection at every tier. DNDO could similarly introduce requirements to detect certain materials, object sizes, shapes, and configurations that could be detected by existing or near-term systems, and increase detection requirements over time by challenging industry to deliver more advanced inspections systems. In this way, the U.S. could meet the 100% scanning requirement by 2018 at "DNDO tier 1", and provide increasing security in subsequent years.

Acknowledgements

This work has been supported by the U.S. Department of Homeland Security (DHS), Domestic Nuclear Detection Office (DNDO), under a competitively awarded contract No. HSHQDC-14-C-B0001 to Rapiscan Laboratories, Inc. This support does not constitute an express or implied endorsement on the part of the Government.

References

Espie, David, 2016, Before the Committee on Transportation and Infrastructure's Subcommittee on Coast Guard and Maritime Transportation and the Committee on Homeland Security's Subcommittee on Border and Maritime Security, July 7. 2016.

CBP, 2017, https://www.dhs.gov/publication/automated-targeting-system-ats-update

Bertozzi, W., Korbly, S.E., Ledoux, R.J., Park, W., Nucl. Inst. Meth. B. 261 (2007) 331-336, "Nuclear resonance fluorescence and effective Z determination applied to detection and imaging of special nuclear material, explosives, toxic substances and contraband"

Areg Danagoulian, William Bertozzi, Curtis L. Hicks Jr., Alexei V. Klimenko, Stephen E. Korbly, Robert J. Ledoux, Cody M. Wilson, 2010, "Prompt Neutrons from Photofission and its use in Homeland Security Applications", 2010 IEEE Conference on Technologies for Homeland Security, November 2010.

Medalia, J-1., 2010, Detection of Nuclear Weapons and Materials: Science, Technologies, Observations, pp. 55-62.

Bertozzi, W., Ledoux, R.J., Nucl. Inst. Meth. B. 241 (2005) 820-825, "Nuclear Resonance Fluorescence imaging in non-intrusive cargo inspection"

Stevenson, J., Gozani, T., Elsalim, M., Condron, C, Brown, C, 2011, Linac based photofission inspection system employing novel detection concepts, Nucl. Ins. Meth. In Phys. Res. 652, 124-128, 2011.

Gary Blanpied, Sankaran Kumar, Dustin Dorroh, Craig Morgan, Isabelle Blanpied, Michael Sossong, Shawn McKenney, Beth Nelson, Material discrimination using scattering and stopping of cosmic ray muons and electrons: Differentiating heavier from lighter metals as well as low-atomic weight materials, Nucl. Inst. Meth., Phys. Res. A 784 (2015) p. 352.

Medalia, J.-2, 2010, Detection of Nuclear Weapons and Materials: Science, Technologies, Observations, pp. 62-76.

Bentley, R. 2016, Test Results for Large-Scale Cargo Inspection Technologies, SORMA Conference (May 2016), and subsequent private communication

Rynes, J., 2015, Approaches to Detect Concealed Threats, Fermi National Laboratory Colloquium, August 2015.

C. Condron, C. Brown, T. Gozani, M. Hernandez, and W.G.J. Langeveld, 2013, "Linear Accelerator X- Ray Sources with High Duty Cycle", AIP Conf. Proc. 1525 (2013) 704.

Tantawi, S., 2015, The Application of Advanced RF Acceleration Technology to Cargo Inspection Systems, Fermi National Laboratory Colloquium, August 2015.

Ogorodnikov, S., Petrunim, V., Vorogushin M. (2002), Proceedings of EPAC 2002, 2807, Paris, France

Arodzero, A., 2015, Accelerator Requirements for Low Dose Advanced Multi-Energy Radiography, Fermi National Laboratory Colloquium, August 2015

Tsahi Gozani et al., "High-Energy X-Ray-Spectroscopy-Based Inspection System and Methods to Determine the Atomic Number of Materials", Patent US 8,750,454 (Issued June 10, 2014).

S. Sinha, J. Kwong, W.G.J. Langeveld, and P. Ryge, 2012, "Characterization of ZnO, BaF2 and PbWO4 scintillator detectors for cargo inspection using transmitted x-ray spectroscopy", Proceedings of the Symposium on Radiation Measurements and Applications (SORMA) 2012, IEEE Trans. Nucl. Sc., 60 (2013) 1016.

W.G.J. Langeveld, C. Condron, M. Elsalim and M. Ingle, 2011, "Noise Spectroscopy: Z determination by Statistical Count-rate ANalysis (Z-SCAN)", Nucl. Inst. Meth. A 652 (2011), 79.

W.G.J. Langeveld, C. Condron, M. Elsalim, P. Grudberg, V. Hu, P. Ryge, T. Shaw, and S. Sinha, 2013, "Implementation of Noise Spectroscopy using biased large-area photodiodes", IEEE Trans. Nucl. Sc., 60 (2013) 937.

WHO, 1990, Food safety aspects relating to the application of X-ray surveillance equipment: Memorandum from WHO meeting, Bull. World Health Org. 31:297-301.

W.G. J. Langeveld, W.A. Johnson, R.D. Owen and R.G. Schonberg, "Intensity Modulated Advanced X-ray Source (IMAXS) for Homeland Security Applications (I)", Proceedings of the Symposium on Radiation Measurements and Applications (SORMA) 2008, IEEE Trans. Nucl. Sc., 56 (2009) 1288.

Bendahan, J., Morton, E. J., Yaish, D., Kolkovich, Y., Goldberg, J., 2016 Systems and Methods for High-Z Threat Alarm Resolution, US 20160216398 A1

U.S. Department of Energy, DoE 1999. Office of Declassification. "Drawing Back the Curtain of Secrecy: Restricted Data Declassification Policy, 1946 to the Present, RDD-1." January 1, 1999. Item V (C) (2) (s)

Medalia, J.-3, 2010, Detection of Nuclear Weapons and Materials: Science, Technologies, Observations, pp. 18, pp. 72.

S&T. 2016,
https://www.dhs.gov/sites/default/files/publications/HME%20Program%20Fact%20Sheet%205OCT16%20508%20Final.pdf